was a heterogeneous mixture of modern-like depleted mantle with a Nb/U ratio of 47 and primitive mantle with a Nb/U ratio of 30. The absence of samples with Nb/U ratios less than the chondritic value supports this interpretation. The source heterogeneity could have formed by incomplete mixing between depleted upper mantle and primitive lower mantle, as predicted by the mantle plume model of (*22*) for greenstones, or simply by variable amounts of continental crust extraction from the primordial upper mantle. In either case, because all initial ε_{Nd} values determined for Lunnon basalts are positive (+2.1 to +3.7) (*12*), including those with Nb/U ratios of ~30 (*23*), this interpretation requires that the subchondritic Nd/Sm ratio of the depleted upper mantle is not related to the formation of the continental crust, as is widely assumed (*5*, *24*). Similarly, continental crust formation could not have been responsible for depleting Th relative to La in the depleted upper mantle because Lunnon basalts, with near-chondritic Nb/U ratios, have subchondritic Th/La ratios (Fig. 1C). The positive initial ε_{Nd} values and subchondritic Th/La ratios of the low Nb/U end-member are consistent with extraction of a now destroyed basalt proto-crust (*25*) from the mantle before formation of the continental crust, assuming, of course, that the basalt proto-crust had a chondritic Nb/U ratio.

REFERENCES AND NOTES

1. A. W. Hofmann, K. P. Jochum, M. Seufert, W. M. White, *Earth Planet Sci. Lett.* **79**, 33 (1986).
2. Incompatible elements are those that partition into the melt phase rather than solid residue during a partial melting event. They have bulk partition coefficients, concentration ratios of an element in the solid residue divided by that in the melt, less than unity.
3. R. L. Rudnick and D. M. Fountain, *Rev. Geophys.* **33**, 267 (1995).
4. E. Anders and N. Grevesse, *Geochim. Cosmochim. Acta* **53**, 197 (1989). The Nb/U ratio estimated for the primitive mantle is based on comparisons with chondritic meteorites.
5. R. L. Armstrong, *Rev. Geophys.* **6**, 175 (1968); *Philos. Trans. R. Soc. London Ser. A* **301**, 443 (1981); *Aust. J. Earth Sci.* **38**, 613 (1991).
6. P. M. Hurley and J. R. Rand, *Science* **164**, 1229 (1969).
7. R. G. Miller, R. K. O'Nions, P. J. Hamilton, E. Welin, *Chem. Geol.* **57**, 87 (1986).
8. S. Moorbath, *ibid.* **20**, 151 (1977); *Philos. Trans. R. Soc. London Ser. A* **288**, 401 (1978).
9. K. P. Jochum, N. T. Arndt, A. W. Hofmann, *Earth Planet Sci. Lett.* **107**, 272 (1991).
10. The Th/U ratios of the mantle sources of MORBs, as calculated from $^{230}Th/^{232}Th$ ratios, are lower than those of OIBs (*11*). Thus, if the Nb/U ratios of MORB and OIB mantle sources are the same, as seems probable (*1*), then their Nb/Th ratios must be different. There is thus considerable uncertainty as to whether the Nb/Th ratio of an ancient basalt reflects crustal extraction alone or has also been affected by whatever process created the Nb/Th differences in the MORB and OIB sources.
11. C. J. Allegre, B. Dupre, E. Lewin, *Chem. Geol.* **56**, 219 (1986); C. Hemond, C. W. Devy, C. Chauvel, *ibid.* **115**, 7 (1994); K. W. W. Sims *et al.*, *Science* **267**, 508 (1995).
12. C. M. Lesher and N. T. Arndt, *Lithos* **34**, 127 (1995).
13. M. T. McCulloch and G. J. Wasserburg, *Science* **200**, 1003 (1978); B. K. Nelson and D. J. DePaolo, *Bull. Geol. Soc. Am.* **96**, 746 (1985); P. J. Patchett and N. T. Arndt, *Earth Planet Sci. Lett.* **78**, 329 (1986); W. Abouchami, M. Boher, A. Michard, F. Albarede, *J. Geophys. Res.* **95**, 17605 (1990).
14. N. T. Arndt and G. A. Jenner, *Chem. Geol.* **56**, 229 (1986).
15. C. Chauvel, B. Dupre, G. A. Jenner, *Earth Planet Sci. Lett.* **74**, 315 (1985).
16. W. Compston, I. S. Williams, I. H. Campbell, J. J. Gresham, *ibid.* **76**, 299 (1986).
17. S. M. Eggins *et al.*, *Chem. Geol.*, in press. In this method of ICPMS, enriched isotope spikes of Li, Sr, Sm, and U are used as internal standards to correct for signal drift. Concentrations of Li, Sr, Sm, and U are determined in the sample unknowns but, unlike in conventional isotope dilution, the measurement is done by external calibration after the contribution of the spike to the normal primary isotope of the element is removed by blank subtraction.
18. A single crustal contaminant cannot produce the two types of enriched basalts. Although Paringa and Devon Consuls basalts have different Nb/U, Nb/Th, La/Sm, and Th/La ratios, consistent with different amounts of crustal contamination by a single contaminant, concentrations of Nb and Sm in the two basalt types are about the same, inconsistent with this interpretation.
19. Initial ε_{Nd} is the deviation of the $^{143}Nd/^{144}Nd$ ratio of a magmatic rock from the chondritic value at the time the rock crystallized.
20. This calculation assumes a hypothetical crustal contaminant with an ε_{Nd} of −5 at 2.7 Ga and a parent magma for the Lunnon basalts with an ε_{Nd} of +3.
21. Lead isotopes are a more sensitive gauge of crustal contamination than Nd and hence, in principle, could be used to distinguish between a primitive mantle and contamination origin for the low Nb/U end-member. Unfortunately, primitive mantle–normalized trace element diagrams for Lunnon basalts are characterized by large positive Pb anomalies, suggesting enrichment in Pb during secondary alteration. Concentrations of Rb, Ba, and Sr, which could provide information about the low Nb/U end-member as well, also have been affected by secondary processes.
22. I. H. Campbell, R. W. Griffiths, R. I. Hill *Nature* **339**, 697 (1989).
23. M. Ghaderi, unpublished data.
24. D. J. DePaolo, *Geophys. Res. Lett.* **10**, 705 (1983).
25. C. G. Chase and P. J. Patchett, *Earth Planet Sci. Lett.* **91**, 66 (1988); S. J. G. Galer and S. L. Goldstein, *Geochim. Cosmochim. Acta* **55**, 227 (1991).

6 August 1996; accepted 15 November 1996

Regulation of NF-κB by Cyclin-Dependent Kinases Associated with the p300 Coactivator

Neil D. Perkins,* Lisa K. Felzien, Jonathan C. Betts, Kwanyee Leung, David H. Beach, Gary J. Nabel†

The nuclear factor κB (NF-κB) transcription factor is responsive to specific cytokines and stress and is often activated in association with cell damage and growth arrest in eukaryotes. NF-κB is a heterodimeric protein, typically composed of 50- and 65-kilodalton subunits of the Rel family, of which RelA(p65) stimulates transcription of diverse genes. Specific cyclin-dependent kinases (CDKs) were found to regulate transcriptional activation by NF-κB through interactions with the coactivator p300. The transcriptional activation domain of RelA(p65) interacted with an amino-terminal region of p300 distinct from a carboxyl-terminal region of p300 required for binding to the cyclin E–Cdk2 complex. The CDK inhibitor p21 or a dominant negative Cdk2, which inhibited p300-associated cyclin E–Cdk2 activity, stimulated κB-dependent gene expression, which was also enhanced by expression of p300 in the presence of p21. The interaction of NF-κB and CDKs through the p300 and CBP coactivators provides a mechanism for the coordination of transcriptional activation with cell cycle progression.

Progression through the eukaryotic cell cycle is controlled by the assembly and activation of specific cyclin-CDK complexes, which provide checkpoints that control entry into each phase of the cell cycle (*1*). Regulation of cyclin-CDK activity is achieved, in part, through the interaction of CDK inhibitory proteins (CKIs) (*2*). Among the CKIs, p21 (also known as WAF1, CIP1, CAP20, or SDI1) is an inhibitor of all CDKs (*2*–*4*). The amount of p21 mRNA and protein is increased upon DNA damage through a mechanism dependent on the tumor suppressor gene p53 (*5*), and p21 is thought to mediate G_1 checkpoint cell cycle arrest (*6*). Synthesis of p21 is also enhanced in cells that are treated with serum factors, phorbol esters, or okadaic acid and undergo growth arrest in a p53-independent manner (*7*, *8*). These latter agents also activate NF-κB (*9*), which regulates genes involved in the response to stress and infection (*10*). Moreover, the induction of either NF-κB or p21 is associated with growth arrest and cellular differ-

N. D. Perkins, L. K. Felzien, J. C. Betts, K. Leung, G. J. Nabel, Howard Hughes Medical Institute, Departments of Internal Medicine and Biological Chemistry, University of Michigan Medical Center, 4520 MSRB I, 1150 West Medical Center Drive, Ann Arbor, MI 48109, USA.
D. H. Beach, Howard Hughes Medical Institute, Cold Spring Harbor Laboratory, Bungtown Road, Cold Spring Harbor, NY 11724, USA.

*Present address: Department of Biochemistry, Medical Sciences Institute, University of Dundee, Dundee DD1 4HN, Scotland, UK.
†To whom correspondence should be addressed.

entiation (*7, 11, 12*). These observations led us to investigate whether the regulation of cell cycle progression may be coordinated with NF-κB transcriptional activation.

To determine whether NF-κB function was influenced by cell cycle regulatory proteins, we cotransfected a eukaryotic expression plasmid encoding p21 into Jurkat T-leukemia cells with a human immunodeficiency virus chloramphenicol acetyltransferase (HIV-CAT) reporter, whose activity is regulated by two κB elements within the long terminal repeat (*13*). Transfection of p21 alone strongly activated HIV-CAT expression in a dose-dependent manner, and mutation of the κB elements within the HIV-1 enhancer nearly abolished this stimulation (Fig. 1A). Cotransfection with an IκB-α expression vector similarly inhibited p21 stimulation, which confirmed that this effect was dependent on constitutive NF-κB (*14*) rather than on an unrelated transcription factor that could bind to the κB site (Fig. 1A). When tested with a multimerized κB site reporter plasmid, mutation of the κB elements again abolished the effect of p21; an unrelated CKI, p16 (*15*), which is functionally active (*16, 17*), only weakly stimulated κB-dependent transcription (Fig. 1B). To confirm that this effect was dependent on the transcriptional activity of NF-κB, we cotransfected cells with p21 and RelA. Both p21 and RelA stimulated HIV-CAT activity when transfected separately. When they were cotransfected, however, the increase in HIV-1 gene expression was more than additive (Fig. 1C). In contrast, p16 poorly enhanced transactivation induced by RelA (Fig. 1D). In an electrophoretic mobility shift assay (EMSA), p21 did not stimulate κB DNA-binding activity. In contrast, Tax or tumor necrosis factor–α (TNF-α), each activators of NF-κB (*18, 19*), induced κB DNA-binding activity in the same experiments (Fig. 1E) (*20*). For these experiments, we used 293 cells because of their high transfection efficiency (>50%), but similar results have been observed in other cell lines (*17*).

These observations suggested that RelA transcriptional activity is stimulated by proteins that inhibit phosphorylation by CDKs. To determine whether there was a biochemical interaction between RelA and CDKs, we examined whether a p21-regulated kinase was associated with RelA (*21*). Associated histone H1 kinase activity was

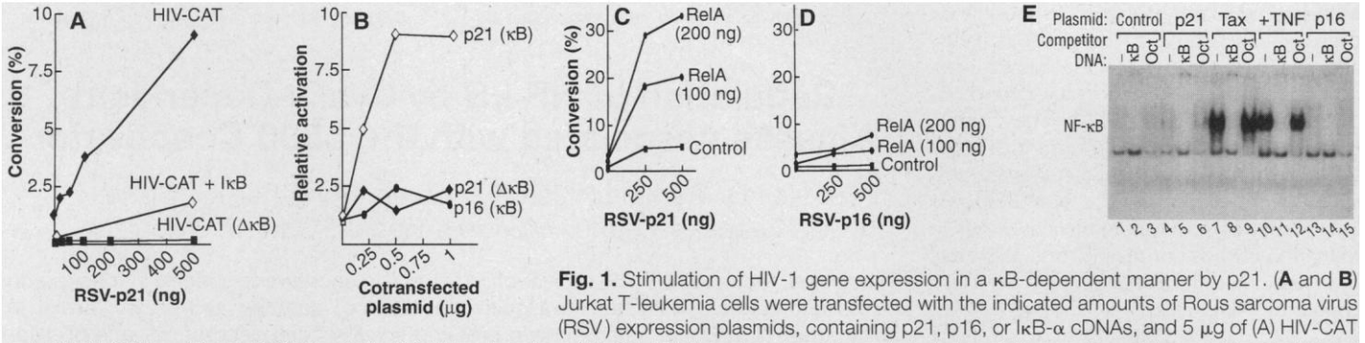

Fig. 1. Stimulation of HIV-1 gene expression in a κB-dependent manner by p21. (**A** and **B**) Jurkat T-leukemia cells were transfected with the indicated amounts of Rous sarcoma virus (RSV) expression plasmids, containing p21, p16, or IκB-α cDNAs, and 5 μg of (A) HIV-CAT or ΔκB HIV-CAT, or (B) 4×κB CAT or 4×ΔκB CAT as described (*13, 14, 18*). A control plasmid was included such that each condition contained a total of 0.5 μg (A) or 1 μg (B) of RSV expression plasmid (*20*). (**C** and **D**) Cooperative induction of HIV-CAT activity by p21 and RelA. Jurkat T-leukemia cells were transfected with HIV-CAT (5 μg) and the indicated amounts of RSV expression plasmids encoding RelA, p21 (C), or p16 (D). A control RSV plasmid was included as necessary so that a total of 0.7 μg of RSV expression plasmid was used. (**E**) EMSA analysis of 293 cells transfected using calcium phosphate with 5 μg of either a control RSV expression plasmid (lanes 1 to 3 and 10 to 12) or expression plasmids encoding p21 (lanes 4 to 6), p16 (lanes 13 to 15), or Tax expression plasmid (lanes 7 to 9). Also, κB DNA-binding activity was induced by incubation with TNF-α (200 U/ml) for 1 hour (lanes 10 to 12). After 44 hours, nuclear extracts (5 μg) were prepared and analyzed with ^{32}P-labeled, double-stranded κB oligonucleotide probe as described (*20*). Unlabeled competitor DNAs (20 ng) were included as indicated.

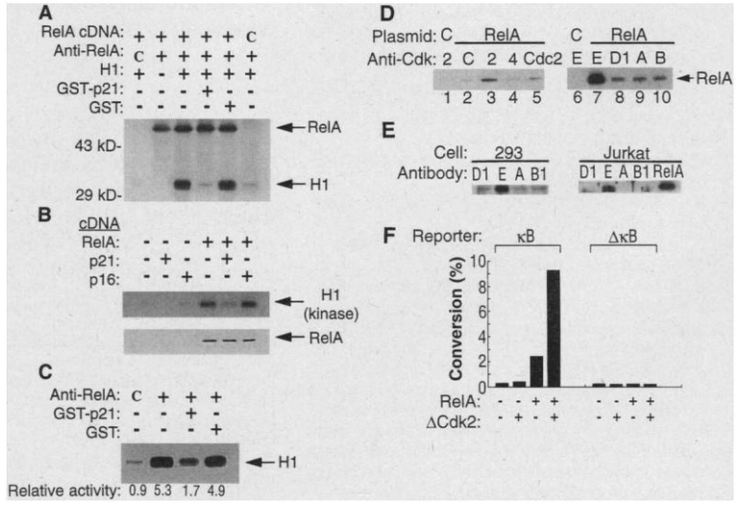

Fig. 2. Biochemical detection of a RelA-associated cyclin E–Cdk2 activity regulated by p21 in vitro and in vivo. (**A** to **E**) The association of a p21-regulated kinase with transfected (A and B) or endogenous (C) RelA was determined by immunoprecipitation of RelA from nuclear extracts as indicated, together with a relevant specified control and subsequent incubation with [γ-^{32}P]ATP and histone H1 (2 μg), as indicated. In (B), all lanes include anti-RelA. Purified GST-p21 or GST (~50 ng) alone (*11*) was included as indicated [(A) and (C)]. Bands corresponding to phosphorylated histone H1 and RelA are labeled. The presence of equivalent amounts of RelA in transfected 293 cells was confirmed by protein immunoblotting in (B). Cyclin or Cdk proteins (Cdk2, Cdk4, or Cdc2) were immunoprecipitated from the relevant nuclear extracts as indicated, and associated RelA was detected by protein immunoblot analysis [in (D) and (E), cyclins are denoted by A, B, D, and E; Cdk2 and Cdk4 are denoted by 2 and 4, respectively]. Nuclear extracts were prepared from control and phorbol ester–stimulated (2 hours) Jurkat T-leukemia cells [(C) and (E)] or TNF-α–stimulated (2 hours) 293 cells (E). Alternatively, nuclear extracts were prepared from 293 cells and transfected as indicated with a cytomegalovirus (CMV) RelA expression plasmid (5 μg) or a CMV control [in (A) and (D)], or CMV RelA expression plasmid (2 μg) and RSV p21, p16, or control expression plasmids (5 μg) [in (B)]. In (D), lane 2 also serves as a control antibody for the right panel (lanes 6 to 10), as these immunoprecipitations were done in the same experiment. (**F**) Enhanced transcriptional activation by RelA in cells transfected with catalytically inactive Cdk2. Jurkat T cells were cotransfected with a multimerized κB or mutant κB reporter plasmid (5 μg), RSV RelA (0.2 μg), and catalytically inactive Cdk2 expression plasmid (0.5 μg) as indicated. Relevant expression plasmid controls were included as necessary.

detected in cells expressing transfected nuclear RelA protein (Fig. 2A). Cotransfection of p21, but not of p16, reduced this RelA-associated kinase activity (Fig. 2B). Although RelA was phosphorylated under these conditions, no change in the overall amount of phosphorylation or in the quantity of RelA itself was noted in the presence of p21 in vitro or in vivo (Fig. 2, A and B) (*17*), which suggested that another kinase may normally phosphorylate RelA through an independent mechanism. Finally, the in vitro histone H1 kinase assay revealed the presence of a putative cyclin-CDK activity associated with endogenous RelA protein from Jurkat cells stimulated with phorbol 12-myristate 13-acetate (PMA) (Fig. 2C). In this experiment, PMA was included as an inducer of NF-κB to facilitate detection of endogenous nuclear RelA protein.

Immunoprecipitation and subsequent protein immunoblot analysis of proteins from RelA-transfected 293 cells revealed that RelA was associated predominantly with cyclin E–Cdk2 complexes in vivo (Fig. 2D). This interaction was also observed with endogenous RelA stimulated by addition of PMA in Jurkat T cells or TNF-α in 293 cells (Fig. 2E). A small amount of RelA was seen associated with Cdc2 and cyclins A, B1, and D1, and less was seen with Cdk4 with available antibodies. The functional importance of Cdk2 kinase activity in the regulation of RelA transactivation was confirmed with the use of a dominant negative, catalytically inactive mutant that causes cell cycle arrest at G_1/S when overexpressed (*22*). Such a mutant would also be expected to stimulate transcription cooperatively when cotransfected with RelA. Consistent with this prediction, the kinase-deficient Cdk2 functioned as a RelA coactivator, similar to p21, and no effect was observed with this gene product on a mutant κB reporter (Fig. 2F). A similar effect was seen when NF-κB was induced by stimulation with TNF-α (*17*).

During immunoprecipitation studies of RelA and its associated CDKs, we observed a large protein associated with these complexes. This protein comigrated with the p300 transcriptional coactivator (Fig. 3A). To confirm its identity, we eluted proteins bound to RelA with high salt and then immunoprecipitated them with antibodies to p300 or to the highly related coactivator CBP (*23*, *24*). Both proteins associated with RelA (Fig. 3B). The p300 protein interacted with endogenous, cellular RelA, as detected by protein immunoblotting after p300 immunoprecipitation from PMA-stimulated Jurkat nuclei (Fig. 3C). The COOH-terminal transactivation domain of RelA apparently was required for this interaction, because no interaction was observed with a truncated RelA protein that contained only the DNA-binding and dimerization domains or when this protein was fused to the heterologous VP16 transactivation domain (Fig. 3D). No interaction was seen with NF-κB1(p50) or with an unrelated transcription factor, Sp1.

We tested whether p300, cyclin E–Cdk2, and RelA associate with one another in vivo. Nuclear extracts prepared from RelA-transfected 293 cells were immunodepleted of p300 or CBP, and then RelA was immunoprecipitated and assayed for histone H1 kinase activity. Depletion of both p300 and CBP decreased RelA-associated H1 kinase activity by ~75% (Fig. 4A). In contrast, depletion with antibodies to other proteins associated with the transcription factor TFIID [including the TATA-binding protein (TBP) and the TFIID subunits $TAF_{II}250$ and $TAF_{II}130$] or the p89 subunit of TFIIH had minimal effect (Fig. 4A). Immunoprecipitates of cellular p300 also contained an active histone H1 kinase that was subject to regulation by p21 but not by p16 (Fig. 4B), and the presence of cyclin E and Cdk2 in this complex was confirmed (Fig. 4C). Similar results were observed with CBP (*17*). These data document the interaction of p300 (or CBP), RelA, and CDKs in vivo.

The biochemical basis for this interaction was shown by immunoprecipitation of in vitro translated p300 with RelA and cyclin E–Cdk2. RelA bound preferentially to the NH_2-terminal region of p300 (Fig. 4D), although a weak, less specific, interaction with the COOH-terminus of p300 was observed (*17*). The interaction of CDK complexes with p300 was also confirmed: Cdk2 complexes bound specifically to the COOH-terminal region of p300 in vitro (Fig. 4E). No interaction was observed between Cdk2 complexes and radiolabeled RelA (Fig. 4F); however, full-length p300 protein facilitated the interaction of RelA and cyclin E–Cdk (Fig. 4A) (*17*). The interaction of RelA with cyclin E–Cdk2 was therefore indirect, with both cyclin E–Cdk2 and RelA binding to separate domains of p300 but not directly to one another.

Finally, we examined the functional role of p300 in transcriptional regulation by NF-κB. Transfection of cells with plasmids encoding p21 and a κB-dependent reporter gene and with increasing amounts of vector encoding p300 stimulated a dose-responsive increase in transcription, and this activity was diminished when a mutant κB reporter gene was used (Fig. 5), which indicated that endogenous NF-κB was required for this effect. Cotransfection of p300 with RelA in

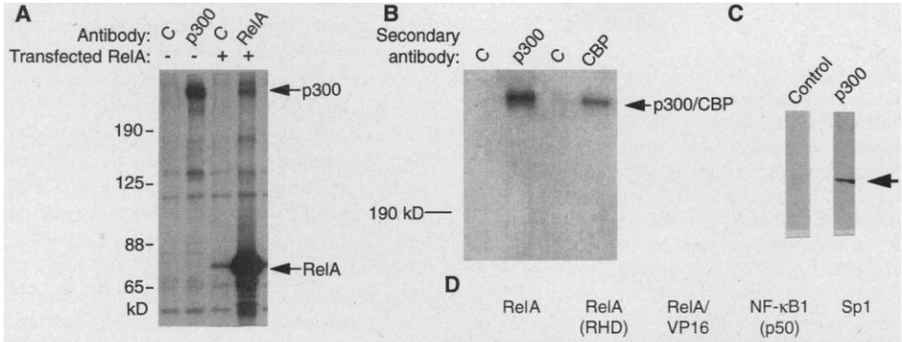

Fig. 3. Association of transcriptional coactivators p300 and CBP with RelA in vivo and in vitro. (**A**) Association of protein with the same mobility as p300 with RelA in vivo. RelA or p300 were immunoprecipitated from nuclear extracts prepared from [^{35}S]methionine-labeled 293 cells transfected with either a CMV RelA expression plasmid or a control, as indicated. Bound proteins were resolved on an SDS polyacrylamide gel (8%). (**B**) Association of p300 and CBP with RelA. RelA was immunoprecipitated as in (A); RelA-associated proteins were then eluted with 300 mM KCl and incubated with anti-p300, anti-CBP, or control antibodies as indicated. Bound proteins were resolved by SDS–polyacrylamide gel electrophoresis (PAGE). (**C**) Association of endogenous NF-κB with p300 in Jurkat cells. RelA(p65)-p300 complexes were detected after immunoprecipitation and protein immunoblot analysis of Jurkat T cells. Nuclear extracts from 3×10^7 Jurkat cells stimulated for 4 hours with PMA were incubated with control antibodies or anti-p300 as indicated. Immune complexes were washed and analyzed by immunoblotting with anti-RelA. (**D**) Specificity and requirement of the RelA transactivation domain for p300 binding. p300 was immunoprecipitated from HL60 extracts and incubated with in vitro translated full-length RelA, the NH_2-terminal Rel homology domain (RHD; amino acids 1 to 306) of RelA, a RelA RHD/VP16 fusion protein, NF-κB1(p50), or Sp1, as indicated. After washing, bound complexes were resolved by SDS-PAGE and detected by ^{35}S autoradiography (I, input translated protein; C, control antibody; +, anti-p300).

the presence of p21 had the same effect (Fig. 5). The magnitude of this effect was comparable to, or greater than, that for interactions of p300 or CBP with other transcription factors (*25*). These results confirm the functional importance of p300 and CDK regulation in NF-κB–dependent gene activation.

Our findings have established that cellular gene activation by NF-κB is affected by signaling that controls cell cycle progression. The p300 protein mediates a biochemical and functional interaction between the RelA subunit of NF-κB and cyclin E–Cdk2. It is probable that inhibitors of CDK activity that act through mechanisms analogous to p21, such as p27 or p57, act similarly on NF-κB. The p300 protein, originally identified as a target for the adenovirus E1A transactivator, associates with the TATA binding protein complex in vivo, is phosphorylated in a cell cycle–dependent manner, is a substrate for CDK proteins in vitro, and is required for the induction of p53-independent p21 gene expression during cellular differentiation (*26*). Further, 12S E1A inhibits NF-κB–dependent gene expression, in contrast to a mutant E1A that is unable to bind p300 (*27*). In addition, overexpression of the COOH-terminus of p300 potentials NF-κB function (*17*). Although p300 and CBP themselves are substrates for CDKs, it is not yet known whether changes in their phosphorylation affect transcriptional coactivation, and it is also possible that p300- or CBP-associated CDKs phosphorylate TBP-associated factors or RNA polymerase II (*28*).

Thus, p300 and CBP serve as multifunctional adapter proteins that coordinate cell cycle progression with NF-κB transcriptional regulation and may be relevant to some other p300- or CBP-associated transcription factors. Rel-related proteins have been implicated in malignancies caused by avian retroviruses and in human lymphomas (*29*). Mutations in CBP and p300 have suggested their possible role in tumorigenesis (*30*). Analysis of knockout strains will help to define the respective functions of these gene products in vivo. Our findings demonstrate the interaction of proteins that control cell cycle progression and the Rel-related family, as well as the importance of p300 or CBP in modulating their activity. The activation of HIV gene expression, regulated by NF-κB, has also been linked to cell cycle progression (*31*). Through their effects on NF-κB transactivation and cell cycle progression, p300 and CBP may potentially influence the activation of HIV gene expression and Rel-related oncogenesis.

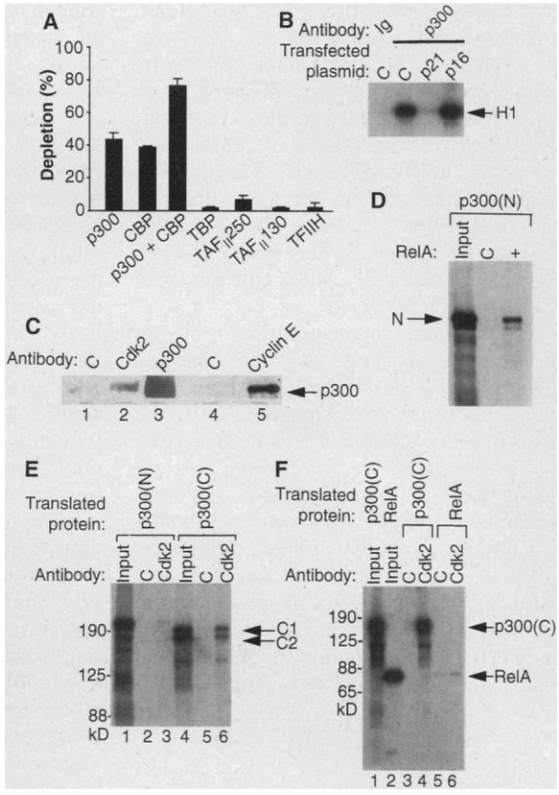

Fig. 4. Biochemical and functional interaction of p300 and cyclin-CDK complexes. (**A**) Association of p300 or CBP with RelA and its Cdk histone H1 kinase activity. Antibodies specific for the indicated transcription factors were prebound to protein G–agarose and incubated with nuclear extracts (100 μg) from 293 cells transfected with RelA. Antibody-bound protein was removed by centrifugation; RelA was then immunoprecipitated, and a histone H1 kinase assay was performed on the RelA-associated proteins. Proteins were resolved by SDS-PAGE and the amount of H1 phosphorylation was quantitated by PhosphorImager analysis. Results are shown as the percentage depletion of activity ± SEM for RelA immunoprecipitated from extracts depleted using a rabbit IgG control and derived from at least three separate experiments. (**B**) Regulation of p300-associated histone H1 kinase activity. Endogenous p300 was immunoprecipitated from 293 cells transfected with control, p21, or p16 expression plasmids as indicated, and a histone H1 kinase assay activity associated with antibody-bound proteins was measured. A mouse IgG2b control was included as indicated. Phosphorylated proteins were resolved by SDS-PAGE. (**C**) Association of p300 with cyclin E and Cdk2 complexes in vivo. Immunoprecipitations were performed with a control antibody (lane 1), anti-Cdk2 (lane 2), or anti-p300 (lane 3) on nuclear extracts from 3×10^7 Jurkat cells that had been stimulated for 4 hours with PMA. Immunoprecipitations with a control antibody (lane 4) or cyclin E mAb (lane 5) were performed with 100 μg of nuclear extract from 293 cells that had been stimulated with TNF-α for 4 hours; p300 was detected by protein immunoblotting with anti-p300. (**D**) Localization of p300 domains required for binding to RelA. RelA was immunoprecipitated from nuclear extracts of 293 cells that expressed transfected RelA and incubated with ^{35}S-labeled in vitro translated NH_2-terminal region of p300 [p300(N); amino acids 1 to 1255]. After washing, bound protein was resolved by SDS-PAGE. Input, 10% input protein; C, control nonspecific rabbit IgG antibody; +, anti-RelA(p65). (**E** and **F**) Binding of Cdk2 complexes to the COOH-terminal region of p300 [p300(C); amino acids 1239 to 2414] but not to RelA. Cyclin-Cdk2 complexes were immunoprecipitated from Jurkat cell nuclear extracts with a control antibody or anti-Cdk2 and incubated with ^{35}S-labeled in vitro p300(N) [(E), lanes 1 to 3] or RelA [(F), lanes 2, 5, and 6] or p300(C) [(E), lanes 4 to 6; (F), lanes 1, 3, and 4] as indicated. Cdk2-bound proteins were resolved by SDS-PAGE (*32*) and detected by ^{35}S autoradiography.

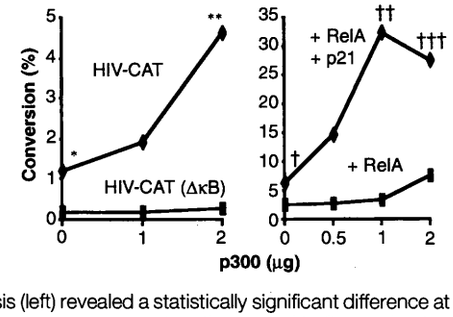

Fig. 5. Functional effects of p300 coactivator and functional coactivation of the HIV enhancer by p300. Jurkat cells were transfected with HIV-CAT or ΔκB HIV-CAT (5 μg) and RSV-p21 (0.5 μg), together with various amounts of the CMV p300 eukaryotic expression vector plasmid as indicated. A control vector with the same CMV regulatory region was included, such that a total of 2 μg of the p300 and control plasmids was present in each sample. Jurkat cells were also transfected with HIV-CAT and RSV-RelA (0.2 μg) in the presence or absence of RSV-p21 (0.5 μg) as indicated. Analysis of the p300 endogenous NF-κB analysis (left) revealed a statistically significant difference at 2 μg of p300 (* versus **, $P = 0.003$ by multiple comparisons contrasting the control to 2 μg using the Scheffe method). For RelA cotransfected with p300, a statistically significant effect was noted at 1 μg, 2 μg, or both († versus ††, $P = 0.002$; † versus †††, $P = 0.005$ by multiple comparisons contrasting the control to 1 or 2 μg using the Scheffe method).

REFERENCES AND NOTES

1. R. W. King, P. K. Jackson, M. W. Kirschner, *Cell* **79**, 563 (1994); K. A. Heichman and J. M. Roberts, *ibid.*, p. 557; C. J. Sherr, *ibid.*, p. 551; P. Nurse, *ibid.*, p. 547.
2. T. Hunter and J. Pines, *ibid.*, p. 573; M. Peter and I. Herskowitz, *ibid.*, p. 181.
3. Y. Gu, C. W. Turck, D. O. Morgan, *Nature* **366**, 707 (1993); J. W. Harper, G. R. Adami, N. Wei, K. Keyomarsi, S. J. Elledge, *Cell* **75**, 805 (1993); A. Noda, Y.

Ning, S. F. Venable, O. M. Pereira-Smith, J. R. Smith, *Exp. Cell Res.* **211**, 90 (1994).
4. Y. Xiong *et al.*, *Nature* **366**, 701 (1993).
5. W. S. El-Deiry *et al.*, *Cell* **75**, 817 (1993); Y. Li, C. W. Jenkins, M. A. Nichols, Y. Xiong, *Oncogene* **9**, 2261 (1994).
6. W. S. El-Deiry *et al.*, *Cancer Res.* **54**, 1169 (1994); A. Di Leonardo, S. P. Linke, K. Clarkin, G. M. Wahl, *Genes Dev.* **8**, 2540 (1994); V. Dulic *et al.*, *Cell* **76**, 1013 (1994).
7. H. Jiang *et al.*, *Oncogene* **9**, 3397 (1994); R. A. Steinman *et al.*, *ibid.*, p. 3389.
8. P. Michieli *et al.*, *Cancer Res.* **54**, 3391 (1994).
9. R. Sen and D. Baltimore, *Cell* **47**, 921 (1986); C. Thevenin *et al.*, *New Biol.* **2**, 793 (1990); A. S. Baldwin, J. C. Azizkhan, D. E. Jensen, A. A. Beg, L. R. Coodly, *Mol. Cell. Biol.* **11**, 4943 (1991); Y. Devary, C. Rosette, J. A. DiDonato, M. Karin, *Science* **261**, 1442 (1993).
10. G. P. Nolan and D. Baltimore, *Curr. Opin. Genet. Dev.* **2**, 211 (1992); M. Grilli, J. J. Chiu, M. J. Lenardo, *Int. Rev. Cytol.* **143**, 1 (1993); U. Siebenlist, G. Franzoso, K. Brown, *Annu. Rev. Cell Biol.* **10**, 405 (1994).
11. G. E. Griffin, K. Leung, T. M. Folks, S. Kunkel, G. J. Nabel, *Nature* **339**, 70 (1989).
12. S. L. Eck, N. D. Perkins, D. P. Carr, G. J. Nabel, *Mol. Cell. Biol.* **13**, 6530 (1993).
13. G. Nabel and D. Baltimore, *Nature* **326**, 711 (1987).
14. C. S. Duckett *et al.*, *Mol. Cell. Biol.* **13**, 1315 (1993).
15. M. Serrano, G. J. Hannon, D. Beach, *Nature* **366**, 704 (1993).
16. G. J. Hannon and D. Beach, *ibid.* **371**, 257 (1994); T. Suzuki, S. Kitao, H. Matsushime, M. Yoshida, *EMBO J.* **15**, 1607 (1996).
17. N. D. Perkins, L. K. Felzien, G. J. Nabel, unpublished data.
18. K. Leung and G. J. Nabel, *Nature* **333**, 776 (1988).
19. L. Osborn, S. Kunkel, G. J. Nabel, *Proc. Natl. Acad. Sci. U.S.A.* **86**, 2336 (1989).
20. W. Lin and L. A. Culp, *Biotechniques* **11**, 344 (1991); N. D. Perkins, A. B. Agranoff, C. S. Duckett, G. J. Nabel, *J. Virol.* **68**, 6820 (1994).
21. Nuclear protein extracts (~125 μg) were incubated at 4°C for 2 hours with anti-RelA (2 μg) (sc-109X; Santa Cruz Biotechnology, Santa Cruz, CA) or control rabbit immunoglobulin G (IgG) in Dignam D buffer [J. D. Dignam, R. M. Lebovitz, R. G. Roeder, *Nucleic Acids Res.* **11**, 1475 (1983)] containing 0.1% NP-40 (adjusted to a final NaCl concentration of 75 mM). Antibody-protein complexes were recovered by incubation for 1 hour with protein G–agarose (10 μl) and low-speed centrifugation. Sedimental material was washed three times with 0.5 ml of incubation buffer [20 mM Hepes (pH 7.9), 75 mM KCl, 2.5 mM $MgCl_2$, 1 mM dithiothreitol (DTT), 0.1% NP-40, 0.5 mM phenylmethylsulfonyl fluoride (PMSF), aprotinin (1 μg/ml), pepstatin A (1 μg/ml), leupeptin (2 μg/ml), and 1 mM sodium vanadate]. For histone H1 kinase assays, protein G–bound complexes were resuspended in 50 μl of kinase buffer [50 mM tris (pH 7.5), 10 mM $MgCl_2$, 1 mM DTT, and 0.5 mM PMSF]. Purified glutathione-S-transferase fusion protein GST-p21 (~50 ng) or GST proteins eluted into kinase buffer containing 10 mM glutathione were added as indicated. The samples were incubated with 133 μCi of [γ-^{32}P]adenosine triphosphate (ATP) and 2 μg of purified histone H1 (Boehringer Mannheim) at 37°C for 15 min with frequent agitation. The reaction was terminated by the addition of SDS gel loading buffer, and a sample was resolved on an SDS-polyacrylamide (15%) gel, which was then dried and subjected to autoradiography. Cyclin-Cdk immunoprecipitations were done as described above for RelA, using 100 or 600 μg of nuclear extract and 10 μg of agarose-conjugated antibodies from Santa Cruz [sc-163AC (Cdk2), sc-601AC (Cdk4), sc-054AC (Cdc2), sc-239AC (cyclin A), sc-245AC (cyclin B1), sc-246AC (cyclin D1), and sc-248AC (cyclin E)]. All antibodies to cyclins were mouse monoclonals (IgG1), the antibodies to Cdk2 and Cdk4 were rabbit polyclonal antibodies to Cdk peptides, and the antibody to Cdc2 was a mouse monoclonal (IgG2a). Protein immunoblotting of RelA was done with a rabbit polyclonal antibody (sc-109, Santa Cruz).
22. S. van den Heuvel and E. Harlow, *Science* **262**, 2050 (1993).
23. Z. Arany, W. R. Sellers, D. M. Livingston, R. Eckner, *Cell* **77**, 799 (1994).
24. Immunoprecipitations and transfections of 293 cells were done as described (Figs. 1 and 2) with antibodies from Pharmingen (14991A for p300 in Fig. 3, A, B, and D) or Santa Cruz [sc-109 (RelA), sc-369 (CBP), and sc-584 (p300 in Fig. 3C)]. Proteins were eluted from RelA (Fig. 3B) by incubation at room temperature for 15 min in wash buffer (*19*) that contained 300 mM KCl and bovine serum albumin (1 mg/ml). Either purified rabbit IgG or mouse IgG2b was used as the control where appropriate. In Fig. 3D, the p300 protein was immunoprecipitated from 200 μg of Jurkat nuclear extract and incubated with the indicated in vitro translated ^{35}S-labeled proteins (TNT rabbit coupled reticulocyte lysate system, Promega). Purified mouse IgG2b was used as the control. Protein association experiments, Bluescript RelA, RelA/VP16, Sp1, NF-κB1(p50), and pET RelA(1–306) plasmids used for in vitro transcription-translation have been described [N. D. Perkins, A. B. Agranoff, E. Pascal, G. J. Nabel, *Mol. Cell. Biol.* **14**, 6570 (1994)].
25. J. R. Lundblad, R. P. S. Kwok, M. E. Laurance, M. L. Harter, R. H. Goodman, *Nature* **374**, 85 (1995); A. J. Bannister and T. Kouzarides, *EMBO J.* **14**, 4758 (1995); R. Janknect and A. Nordheim, *Oncogene* **12**, 1961 (1996); P. Dai *et al.*, *Genes Dev.* **10**, 528 (1996).
26. P. Yaciuk and E. Moran, *Mol. Cell. Biol.* **11**, 5389 (1991); S. E. Abraham, S. Lobo, P. Yaciuk, H. H. Wang, E. Moran, *Oncogene* **8**, 1639 (1993); R. Eckner *et al.*, *Genes Dev.* **8**, 869 (1994); A. C. Banerjee *et al.*, *Oncogene* **9**, 1733 (1994); C. Missero *et al.*, *Proc. Natl. Acad. Sci. U.S.A.* **92**, 5451 (1995).
27. A. M. Ventura, M. Q. Arens, A. Srinivasan, G. Chinnadurai, *Proc. Natl. Acad. Sci. U.S.A.* **87**, 1310 (1990); H. G. Wang *et al.*, *J. Virol.* **67**, 476 (1993); C. Song, P. M. Loewenstein, M. Green, *ibid.* **69**, 2907 (1995); S. F. Parker, L. K. Felzien, N. D. Perkins, M. J. Imperiale, G. J. Nabel, *J. Virol.*, in press.
28. R. Roy *et al.*, *Cell* **79**, 1093 (1994); R. Shiekhattar *et al.*, *Nature* **374**, 283 (1995); S.-M. Liao *et al.*, *ibid.*, p. 193; H.-P. Gerber *et al.*, *ibid.*, p. 660.
29. T. D. Gilmore and H. M. Temin, *Cell* **44**, 791 (1986); A. Neri *et al.*, *ibid.* **67**, 1075 (1991).
30. F. Petrij *et al.*, *Nature* **376**, 348 (1995); M. Muraoka *et al.*, *Oncogene* **12**, 1565 (1996).
31. J. He *et al.*, *J. Virol.* **69**, 6705 (1995); J. B. M. Jowett *et al.*, *ibid.*, p. 6304; S. R. Bartz, M. E. Rogel, M. Emerman, *ibid.* **70**, 2324 (1996).
32. The antibodies to p300 used were 14991A (Pharmingen) and sc-584 (Santa Cruz); the antibodies to CBP, TBP, $TAF_{II}250$, $TAF_{II}130$, TFIIH p89 subunit, Cdk2, cyclin A, cyclin B1, and cyclin E were from Santa Cruz (sc-369, sc-204, sc-735, sc-736, sc-293, sc-163, sc-239AC, sc-245AC, and sc-248AC, respectively). The p300 cDNAs were obtained by polymerase chain reaction (PCR) amplified with the EXPAND PCR kit (Boehringer) from polyadenylated RNA (0.5 μg) from human spleen (Clontech) with oligo(dT) as a primer and reverse transcriptase (Stratagene). A 5′ fragment (sense, 5′-GCTAAGCTTCACCATGGCCGAGAATGTGGTGGAACCGGGGCCG-3′; antisense, 5′-CACAGATCTGATGCATCTTTCTTCCGCACTCTGTAC-3′), as well as a 3′ p300 fragment overlapping the internal Bgl II site (sense, 5′-ATCAGATCTGTGTCCTTCACCATGAGATCATCTGGC-3′; antisense, 5′-GCTAGATCTCTAGTGTATGTCTAGTGTACTCTGTGAGAGG-3′) were isolated and subcloned into pBluescript downstream of the T7 promoter.
33. We thank D. Gschwend for secretarial assistance; N. Barrett and K. Carter for preparation of figures; G. Hannon for p21 and p16 plasmids; P. Hobart (Vical Inc.) for the VCL-1012 CMV expression plasmid; G. Enders, J. LaBaer, and E. Harlow for the dominant negative Cdk2 plasmid; and W. Kong, Z. Yang, S. Parker, and other members of the Nabel lab for their advice and comments. N.D.P. is the recipient of a Scholar Award from the American Foundation for AIDS Research (AmFAR) in memory of James Hoese. Supported in part by NIH grant RO1 AI29179.

15 July 1996; accepted 25 November 1996

A Legume Ethylene-Insensitive Mutant Hyperinfected by Its Rhizobial Symbiont

R. Varma Penmetsa and Douglas R. Cook*

Development of the *Rhizobium*-legume symbiosis is controlled by the host plant, although the underlying mechanisms have remained obscure. A mutant in the annual legume *Medicago truncatula* exhibits an increase of more than an order of magnitude in the number of persistent rhizobial infections. Physiological and genetic analyses indicate that this same mutation confers insensitivity to the plant hormone ethylene for multiple aspects of plant development, including nodulation. These data support the hypothesis that ethylene is a component of the signaling pathway controlling rhizobial infection of legumes.

In contrast to pathogenic plant-microbe interactions where persistent infection is correlated with cellular dysfunction and disease, compatible rhizobia trigger morphogenesis of a nodule organ and symbiotic nitrogen fixation on their legume host plant. Despite the beneficial aspects of this symbiosis, rhizobial infection is regulated by the plant host. One mechanism for controlling infection by compatible rhizobia, referred to as feedback inhibition of nodulation, is evidenced as a transient susceptibility to rhizobial infection in root hair cells (*1*). This transient susceptibility results in a narrow zone of infection and nodule differentiation (Fig. 1A). Plant mutants defective in feedback inhibition of nodulation continue to produce nodules from newly developed root tissue (*2*). A possible second mechanism for controlling rhizobial infection involves the early arrest of rhizobial infections within the nodulation zone; in fact, only a minority of rhizobial infections

Department of Plant Pathology and Microbiology, Crop Biotechnology Center, and Graduate Program in Genetics, Texas A&M University, College Station, TX 77843, USA.

*To whom correspondence should be addressed.